

Vortex-induced reconfiguration of a tandem arrangement of flexible cylinders

Sang Joon Lee^{*}, Jeong Jae Kim^a and Eunseop Yeom^b

Department of Mechanical Engineering, Pohang University of Science and Technology (POSTECH), San 31,
Hyojadong, Pohang 790-784, South Korea

(Received November 19, 2014, Revised February 26, 2015, Accepted March 19, 2015)

Abstract. Oscillating motions of flexible cylinders are associated to some extent with the aerodynamic response of plants. Tandem motions of reeds with flexible stems in a colony are experimentally investigated using an array of flexible cylinders made of polydimethylsiloxane (PDMS). Consecutive images of flexible cylinders subjected to oncoming wind are recorded with a high-speed camera. To quantify oscillating motions, the average bending angle and displacement of flexible cylinders are evaluated using point-tracking method and spectral analysis. The tandem motions of flexible cylinders are closely related to the flow characteristics around the cylinders. Thus, the dynamic motions of a tandem arrangement of flexible cylinders are investigated with varying numbers of cylinders arranged in-line, numbers of cylinders in a group (behaving like a single body), and Reynolds numbers (Re). When the number of cylinders in a group increases, the damping effect caused by the support of downstream cylinders is pronounced. These results would provide useful information on the tandem-arranged design of complex structures and energy harvesting devices.

Keywords: flexible cylinder; tandem arrangement; in-line cylinders; reconfiguration

1. Introduction

Mechanical interactions between wind and plants, particularly flexible vegetation that develop streamlined postures to reduce the projected area perpendicular to oncoming flow when subjected to wind, have been investigated for a long time. Compared with rigid and upright vegetation, this reconfiguration of flexible vegetation leads to a significant reduction in drag force (Vogel 1989). Alben *et al.* (2002) and Gosselin *et al.* (2010) explained how the reconfiguration of flexible bodies changes the drag or restoring force exerted on flexible vegetation.

Oscillating motions of flexible cylinders are known to be associated to some extent with the aerodynamic response of plants. The effect of wind on plant motion and the damped oscillation of giant reeds were analyzed by de Langre (2008) and Speck and Spatz (2004). However, there is no systematic study that uses flexible cylinders in tandem arrangements to understand the reconfiguration of flexible real plants. Dynamic behaviors of flexible cylinders with respect to

*Corresponding author, Professor, E-mail: sjlee@postech.ac.kr

^a Mr., E-mail: simple1022@postech.ac.kr

^b Mr., E-mail: yesgood@postech.ac.kr

oncoming wind can be roughly explained based on the flow information around the cylinders.

Many studies were conducted on the characteristic structure of flow around rigid cylinders and the vortex-induced structural vibration by Bearman (1984), Sarpkaya (2004), and Williamson and Govardhan (2004). The flow behind multiple-cylinder configurations has complex interactions among the wakes, vortices, shear layers, and Karman vortex streets. For multiple cylinders arranged in a line, numerous experimental studies were conducted under steady cross-flow conditions. Among these studies, two circular cylinders arranged in various configurations were investigated by Zdravkovich (1977) and a review article on this topic was written by Sumner (2010). In addition, the flows around three cylinders arranged in-line (Aiba and Yamazaki 1976), four cylinders in-line (Igarashi 1986, Igarashi and Suzuki 1984), and five cylinders in-line (Hetz *et al.* 1991) were investigated.

Unlike rigid cylinders, flexible cylinders move according to complex flow–structure interactions. Huera-Huarte and Bearman (2009) reported that the dynamic responses, including displacement and dominant frequency, of a long flexible cylinder are caused by vortex-induced vibration. Depending on the gap distance between adjacent cylinder models and the reduced velocity, the response of the trailing cylinder is affected by vortex-induced vibrations, wake-induced vibrations, or their combination (Huera-Huarte and Bearman 2011, Huera-Huarte and Gharib 2011). However, previous studies about flexible cylinders mainly focused on the offshore engineering applications by testing long oil pipelines fixed at two ends which vibrate at high frequencies. Therefore, these previous studies cannot be applied to understand the oscillatory motion of flexible plants fixed only at the bottom, because the dynamic behaviors of flexible plants such as reed colony are quite different from those of previous studies.

In the present study, the oscillating motions of flexible cylinders arranged in tandem configuration were investigated with varying Reynolds number (Re) to understand the reconfiguration of reeds with flexible stem. Compared with a single cylinder, two or three cylinders in tandem arrangement have a more damped oscillating motion because they behave as a single body. The oscillating motions of a group of flexible cylinders were quantitatively analyzed by measuring the average bending angle and displacement using point tracking technique and spectral analysis. As the number of flexible cylinders arranged in-line increased from three to five, interesting tandem motions of flexible cylinders occurred because of the peculiar flow characteristics around the cylinders. These results could be bio-mimicked in the design of high-rise structural complexes.

2. Methods and materials

2.1 Experimental setup in a wind tunnel

Experiments were conducted in a closed-return type wind tunnel with a test section of 0.72 m × 0.65 m × 8 m (W × H × L) (Fig. 1(a)). Wind velocity was monitored using a Pitot tube installed at the test section. Wind velocity in the test section was increased from 3 m/s to 8 m/s in increments of 0.5 m/s. Two-dimensional oscillating motions of flexible cylinders were recorded by a high-speed camera (Ultima-APX, Photron, Japan) at a frame rate of 125 fps for 8.19 s. An Xe lamp was employed as illumination source (Fig. 1). The stream wise pressure gradient was nearly negligible because of the presence of corner fillets and small adjustable breathers located between the wind tunnel test section and the first diffuser. Mean stream wise velocity was normalized by

the reference velocity at the top of the cylinder model.

2.2 Flexible cylinder model

The diameter of each flexible cylinder model made of polydimethylsiloxane (PDMS) was $D = 5.8$ mm. Length (l) and aspect ratio (l/D) of the model were 0.13 m and 22.41 respectively (Table 1). Re was defined based on the diameter of PDMS cylinder model. The flexible cylinder models were mounted on an acrylic holder with holes of 5.8 mm in diameter. In the present experiment, the cylinder models were arranged in-line parallel to the wind direction. The number of cylinders in the in-line configuration ranged from one to five, with an inter-cylinder spacing of 15 mm ($2.6D$). All PDMS cylinder models were coated with black spray paint to reduce their surface interactions and to easily distinguish their motions with high image contrast. The effect of black color coating on the structural properties of the PDMS cylinders was negligible.

2.3 Measurement of oscillating motions of flexible cylinders

Oscillating motions of flexible cylinders were analyzed using digital image processing techniques. Each image was converted into a binary image by thresholding with an optimal value determined by using Otsu's algorithm. For quantitative comparison of these oscillating motions, the bending angle and displacement (y) of cylinders were evaluated. Here, the bending angle is defined as the angle between the vertical axis and the inclined line connecting the specific point 2.5 cm above the bottom and the tip of the deflected cylinder (Fig. 1(b)).

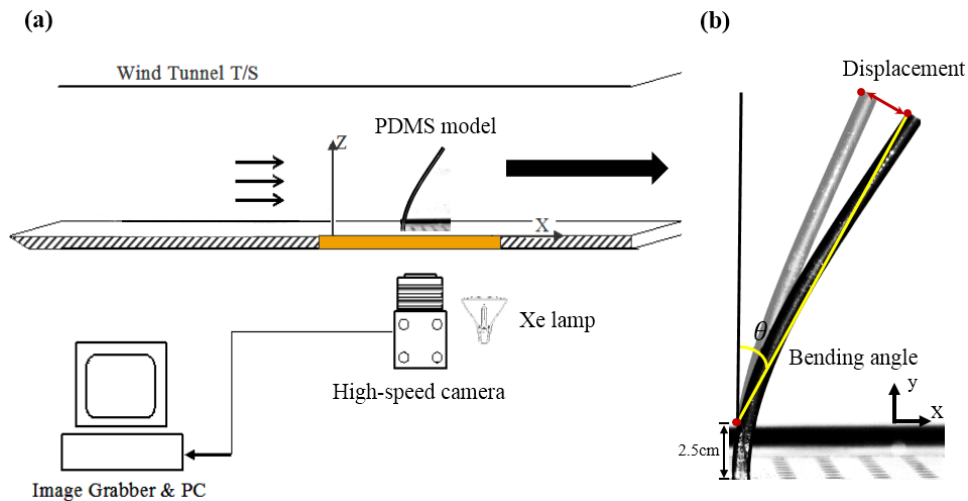


Fig. 1 (a) Schematics of the experiment setup composed of a wind tunnel, a high-speed camera, an Xe lamp, a PC, a Pitot tube, and a micromanometer. (b) Representation of bending angle (θ) and displacement of an oscillating cylinder. Bending angle is defined as the angle between vertical axis and inclined line connecting the specific point 2.5 cm above the bottom with the tip of the deflected cylinder. Displacement is evaluated as the distance moving from the tip of the reference cylinder. For easy understanding, the image of the reference cylinder is superimposed on the image of the deflected cylinder

Table 1 Experiment parameters used in the present study

| | | | |
|----------------------|-----------------|------------------|------------------------|
| Length | L | m | 0.13 |
| Diameter | D | m | 0.0058 |
| Aspect ratio | l/D | — | — |
| Young's modulus | E | N/m ² | — |
| Reynolds number | UD/ν | — | 1150–3070 |
| Kinematic viscosity | ν | — | 15.11×10^{-6} |
| Wind speed | U | m/s | 3–8 |
| Displacement | y/D | — | — |
| Bending angle | θ | ° | — |
| Drag reduction ratio | $AC_D/(AC_D)_0$ | — | ≤ 1 |

Mean bending angle of the first cylinder in a cylinder array is used as a representative parameter because the tips of the flexible cylinders exhibit oscillatory motion. The displacement of each cylinder was measured by tracking its tip. Displacement (y) between the first and subsequent images exhibited a periodic variation because of the oscillation motion of the cylinder. Mean normalized displacement (y/D) was used to compare the oscillating motions of flexible cylinders.

2.4 Drag reduction ratio

To compare the oscillation motions of flexible cylinders, average displacement and average bending angle with varying experimental parameters were evaluated (Table 1). Average bending angle of a cylinder is related to the drag force exerted on the cylinder. From the average bending angle data, the drag reduction ratio [$AC_D/(AC_D)_0$] can be estimated by using the following equation

$$AC_D/(AC_D)_0 = \cos^2\theta \quad (1)$$

where A , C_D , $(AC_D)_0$, and θ are the surface area, drag coefficient, surface area multiplied by the drag coefficient without bending, and bending angle of the cylinder, respectively. The bending of a flexible cylinder gives rise to a reduction of drag force because of a decrease in projection area.

3. Results and discussion

3.1 Similarity between reed and PDMS cylinder

Fig. 2 compares the bending behaviors of a representative giant reed (*Arundo donax*) and a PDMS cylinder subjected to wind speed increasing from 3 m/s to 8 m/s in increments of 1 m/s. For a clear comparison of bending behaviors, average bending angles of the reed and PDMS cylinder

as a function of Re were compared (Fig. 2(c)). There are many factors affecting the dynamic behaviors of a flexible cylinder, such as material property, structural configuration, aspect ratio, and mass. Thus, the relationship between the bending angle and Re was dealt with an important factor rather than the absolute values of bending angle. The slope of their bending angles with respect to Re are similar each other (reed = 0.0135, PDMS cylinder = 0.0106). This seems to be attributed to their similar Young's modulus: PDMS cylinders = 0.36–0.87 GPa, giant reed (*Arundo donax*) = 0.3–1.0 GPa (Spatz *et al.* 1997). The slopes were evaluated from the fitting curves in the range of Reynolds number $1150 \leq Re \leq 3070$, depicted in Fig. 2(c). The change of Re indicates the changes of wind speed and the corresponding force exerting on the cylinder. Thus, the slope of bending angle with respect to Re represents the ratio of the change in the exerting force to that in the bending angle. Because this ratios for the PDMS cylinder and the reed are similar each other, the change in the bending angle of reeds in groups can be depicted by the change in the bending angle of the PDMS cylinders, when the exerting force on the cylinder is changed by upstream or downstream cylinders. Based on these results and assumptions, PDMS cylinder was selected as a bio-mimicking model of giant reeds to investigate the group oscillation motion of reed colony in the present study.

3.2 Results of a single PDMS cylinder

A single flexible PDMS cylinder bends up to a specific bending angle and then oscillates under constant wind speed. Temporal variation of displacement of the oscillating single cylinder was analyzed. Fig. 3(a) shows consecutive images of an oscillating cylinder at specific instants from t_0 to t_7 at $Re = 3071$. The corresponding displacement changed periodically as shown in Fig. 3(b). Fast Fourier transform analysis was performed on all displacement data collected in 8.19 s, and then the dominant frequency and amplitude information were obtained (Fig. 3(c)). Average bending angle and average displacement were statistically analyzed to compare the oscillating motions according to Re (Fig. 4). The average bending angle and displacement are linearly increased as the wind speed increases. This results reveal that these two parameters well represent the bending and oscillating motions of a single cylinder according to wind velocity.

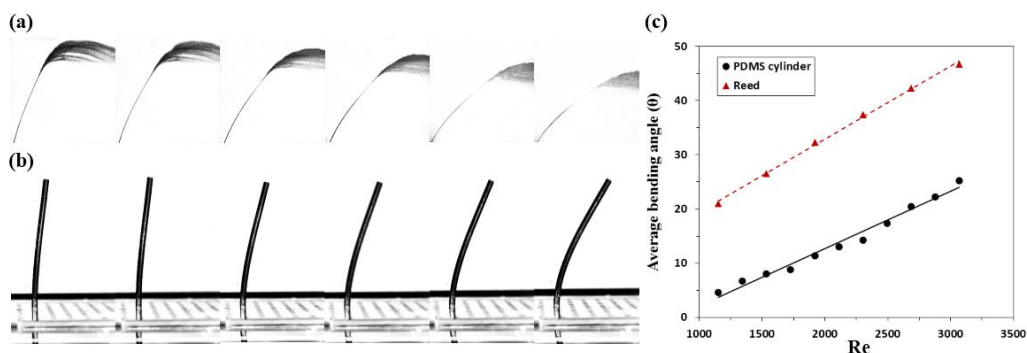


Fig. 2 Sequential images showing the bending behaviors of a reed and a PDMS cylinder. The bending tendency of (a) the reed and (b) the PDMS cylinder as the wind velocity increases from 3 m/s to 8 m/s at increments of 1 m/s. Wind direction is from left to right. (c) Variation of average bending angle with respect to Re . Dashed and solid lines represent the linear-curve fitting of the average bending angle with respect to Re for the reed and PDMS cylinder

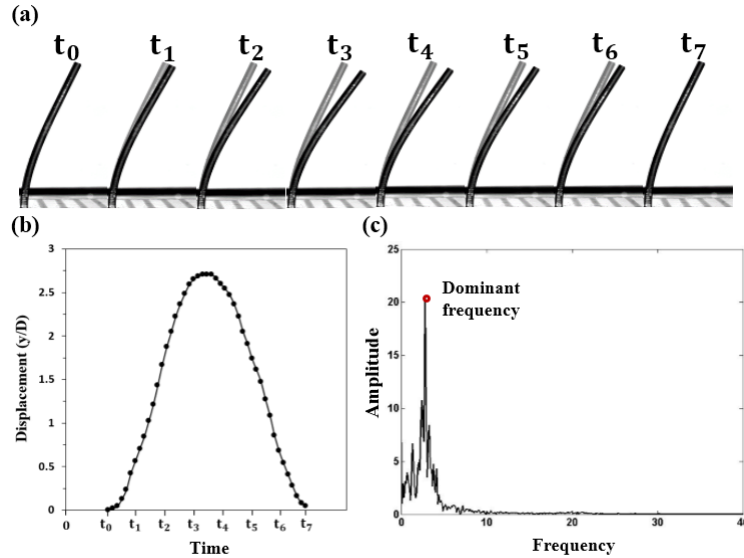


Fig. 3 (a) Oscillating motion of a single PDMS cylinder at a wind velocity of 8 m/s in a cycle (t_0 - t_7), The reference cylinder at t_0 is superimposed on all cylinders for easy comparison, (b) Cyclic variation of displacement of the tip of the deflected cylinder, (c) Dominant frequency in spectral domain

3.3 Tandem configuration of two and three cylinders

Tandem configuration was observed when two or three cylinders were arranged in-line. As shown in Fig. 5, this tandem configuration gives rise to slightly different bending and oscillating motions. When two cylinders are arranged in tandem, the downstream cylinder is less affected by the oncoming wind than the upstream cylinder because of the reduction of wind speed by the upstream cylinder (Sumner, 2010). The different bending angles of the upstream and downstream cylinders cause their tips to come into contact with each other. After the contact, the cylinders move together as a group (Fig. 5(a), middle). In accordance with the findings of Zdravkovich (1987), Xu and Zhou (2004), and Zhou and Yiu (2006), the free shear layer separated by the upstream cylinder overshoots the downstream cylinders when they are in the extended-body regime, where the distance between the two cylinders ranges from $1D$ to $2D$ (Fig. 6(a)). Thus, the downstream cylinder is not affected by the vortices shed from the upstream cylinder in the extended-body regime. Actually, the two cylinders oscillate together without detachment owing to the presence of the free shear layers surrounding them.

When three cylinders are arranged in-line, two different tandem configurations are observed (Fig. 7(a)). In the first configuration, all three cylinders oscillate as a group (Fig. 5(a), bottom). Similar to the tandem configuration of two cylinders, all three cylinders behave like a single body when they are in the extended-body regime. In the second configuration, three cylinders oscillate separately in two groups composed of two upstream cylinders and one downstream cylinder. The latter case will be discussed in the next section.

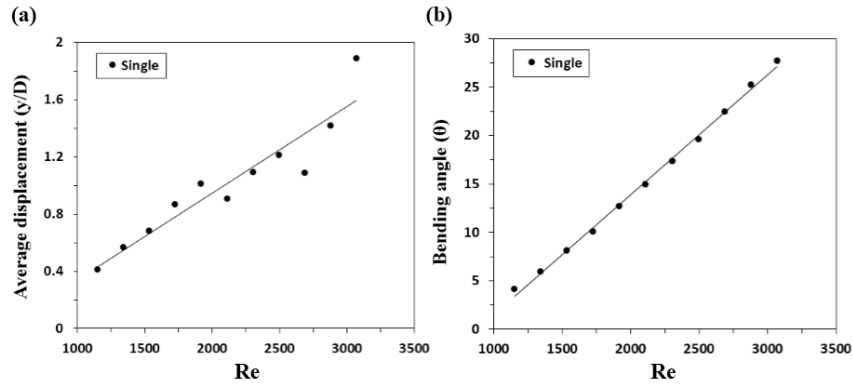


Fig. 4 Variation of (a) bending angle and (b) average displacement with respect to Re of a single PDMS cylinder

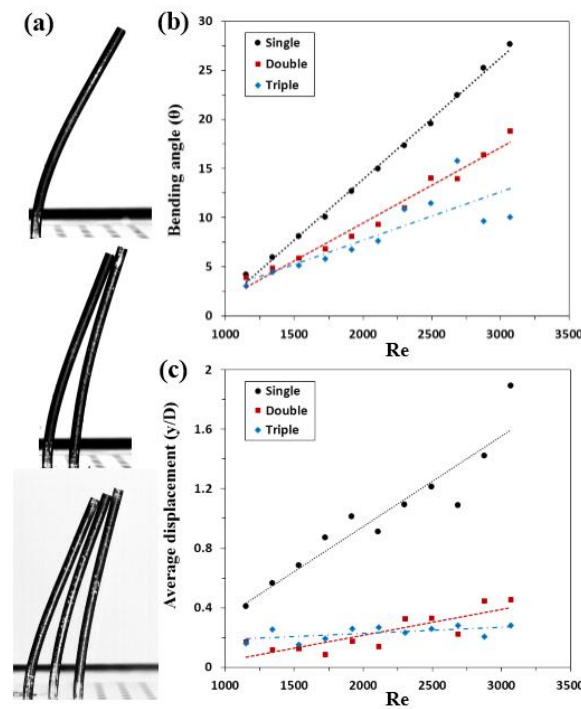


Fig. 5 (a) Reconfigurations of single, two, and three cylinders arranged in-line at $Re = 3071$. Variations of (b) mean bending angle (θ) and (c) average displacement (y/D) with respect to Re

Figs. 5(b) and 5(c) compare the average bending angle and average displacement of single, two, and three cylinders arranged in line. The bending angles for all cases are linearly increased according to Re . The variation tendency of average displacement for a single cylinder is distinctly higher than that for the other two cases. When Re is larger than 2301, the average displacement of the three-cylinder group is smaller than that of the two-cylinder group. However, the average

displacement exhibits just the opposite when Re is less than 2301.

When Re is equal to 1535, the two upstream cylinders among the three cylinders start to form a group. Therefore, the displacement of the remaining downstream cylinder increases because the vortices shed from the two upstream cylinders results in the downstream cylinder being positioned either in or out of the extended-body regime. Once the shear layer that separated from the upstream cylinders encloses the downstream cylinder (Re is larger than 2301), the three cylinders will be positioned in the extended-body regime and will behave as a single bluff body. Slight variations in average bending angle and average displacement seem to be related to these different tandem configurations of three cylinders depending on Re .

When the cylinders are grouped as a single structure, their stiffness is increased. The increase of stiffness implies that additional force is required to achieve the same bending angle. As mentioned in the previous section, the slope of bending angle with respect to Re represents the ratio of the change in the exerting force to that in the bending angle. Therefore, the increased stiffness reduces the slope of bending angle with respect to Re , as depicted in Fig 5(b). The displacement of multiple cylinders in group is also reduced due to their increased stiffness.

In addition, the downstream cylinders support the deflected upstream cylinder with providing damping effect on the displacement of the upstream cylinder, because the fixed bottom gap between the cylinders is larger than the distance between cylinder tips (Fig. 5(a)). Thus, the significant reduction in average displacement of tandem cylinders (Fig. 5(c)) can be explained by the mass–spring–damper system expressed by the following equation:

$$m\ddot{y} + c\dot{y} + ky = f(t) \quad (2)$$

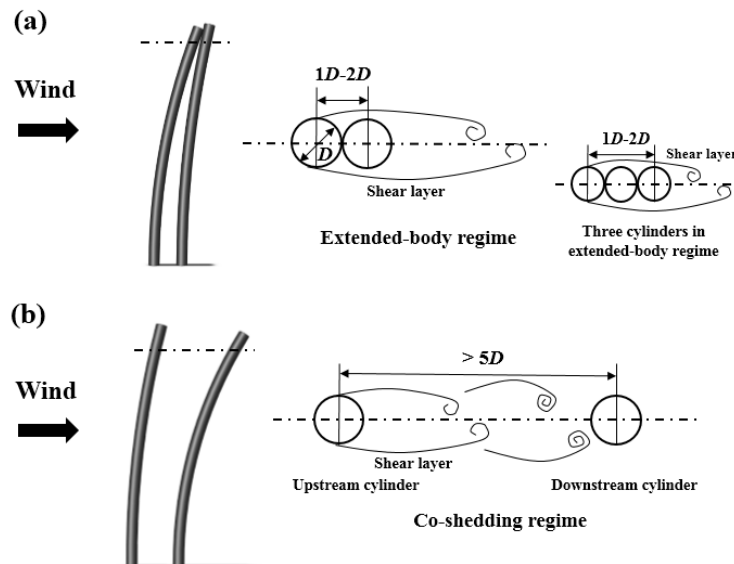


Fig. 6 Two different flow patterns around two cylinders in tandem arrangement, (a) Flow around two and three cylinders in tandem arrangement in the extended-body regime, (b) Flow patterns around two cylinders in the co-shedding regime

where m , c , and k are the mass, damping coefficient, and stiffness, respectively. Solution y represents the displacement of the cylinder. Assuming that the wind load $f(t)$ is constant at a given wind velocity, the average displacement can be compared with the experiment results. A single cylinder exhibits harmonic oscillation ($c = 0$) because it has no damping effect. However, when two or three cylinders are grouped, the cylinders located behind the first upstream cylinder work as a damper. The two and three cylinders arranged in tandem configurations exhibit damped harmonic oscillation when wind speed is constant. The ratio of average displacement of the two- and three-cylinder groups is about 1.5 when three cylinders are in the extended-body regime. Solving Eq. (2) results in a damping coefficient of the three-cylinder group that is twice that of the two-cylinder group.

3.4 Three oscillation modes of multiple cylinders

When the number of cylinders in tandem arrangement is more than three, they are divided into groups that show distinct oscillating motions. Fig. 7 illustrates three different configuration modes of multiple cylinders arranged in-line.

The first configuration mode occurs when Re is relatively low ($Re \leq 1550$). As previously discussed in section 3.3, the two upstream cylinders that form a group under this Re range fall within the extended-body regime. However, the downstream cylinders sway separately (Mode 1 in Fig. 7). The downstream cylinders are largely influenced by the vortices shed from the upstream cylinders. The shear layer that separated from the upstream cylinders is not so strong in the downstream region with low Re condition. Therefore, the downstream cylinders are affected by both large-scale vortices and wind-speed reduction because of the presence of upstream cylinders. In this region, the downstream cylinders are observed to have small displacement in low Re condition. As the number of downstream cylinders increases, the effect of wind-speed reduction is enhanced, causing smaller displacement of the downstream cylinders.

In the second configuration mode, the cylinders in tandem arrangement are divided into groups of two (double) or three (triple) cylinders that exhibit damped oscillating motions. The second mode of the three cylinders arranged in-line shows two different types of configuration (Fig. 7). Three cylinders move in tandem as a group and are then divided into two groups: two upstream cylinders and one downstream cylinder (Mode 2 in Fig. 7). As discussed in the first mode, the two upstream cylinders form a group first in low Re . The downstream cylinder is affected by vortices shed from the two upstream cylinders. The distance between the two upstream cylinders and the downstream cylinder is changed by the displacement of the downstream cylinder. The downstream cylinder can be one of those positioned in the co-shedding regime when the distance between cylinders exceeds $5D$ (Fig. 6(b)) and in the extended-body regime. As the shear layer separated from the upstream cylinders overshoots over the downstream cylinder, they move together as discussed in the previous section. Once the downstream cylinder falls within the co-shedding regime, the downstream cylinder is largely affected by the vortices shed from the upstream two cylinders. Its motion is independent of the two upstream cylinders. The second type of configuration is observed more often than the first type of configuration in three cylinders arranged in-line.

When four cylinders are in an in-line configuration, the third and fourth cylinders form a group because the second type of configuration of three cylinders occurs frequently. As the shear layer separated from the third cylinder overshoots the downstream fourth cylinder, the downstream two cylinders form another group. Thus, four cylinders arranged in-line are divided into two groups

consisting of two upstream cylinders and two downstream cylinders (Mode 2 in Fig. 7(b)). When five cylinders are in an in-line configuration, the two groups consisting of two upstream cylinders and the two downstream cylinders are formed at first, as shown in the four-cylinder configuration. The last fifth cylinder is not positioned inside the shear layer separated from the two downstream cylinders. Therefore, it moves in a different phase with the two frontal groups. The five cylinders are divided into three groups, consisting of two upstream cylinders, two downstream cylinders, and the last cylinder (Mode 2 in Fig. 7(c)).

Mode 3 configuration appears at a high Re number, mostly $2880 \leq Re \leq 3081$. In Mode 3, all cylinders oscillate randomly with very large amplitude in a three-dimensional (3D) manner. Motion analysis for Mode 3 was excluded in this study because 3D oscillation induces complex flow structures. Although the 3D motion of cylinders is important, it does not have a significant influence on the average bending angle and displacement of a group of cylinders arranged in-line.

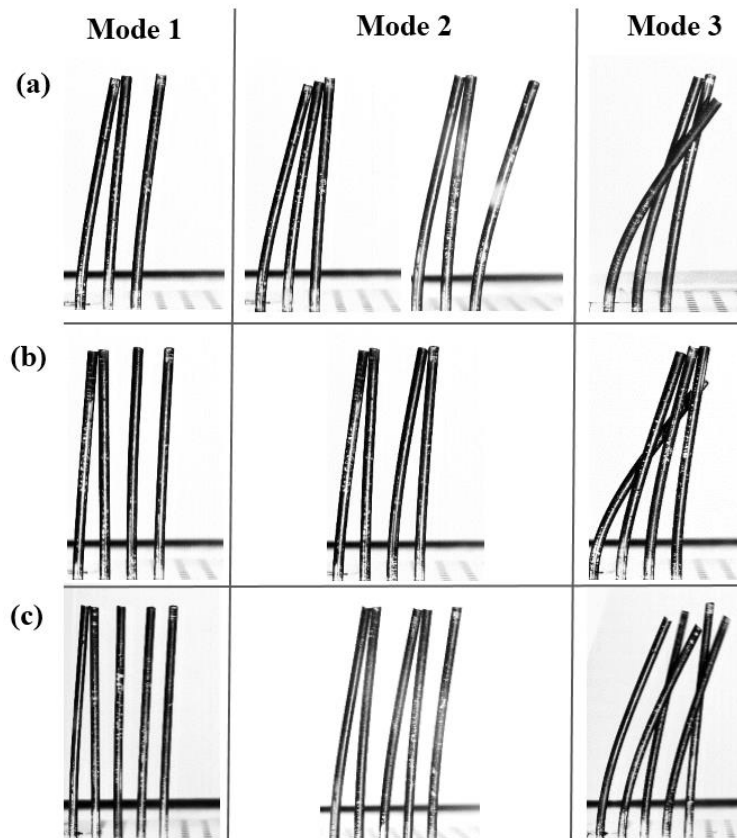


Fig. 7 Three different modes of configuration for (a) three cylinders, (b) four cylinders, and (c) five cylinders arranged in-line according to wind speed. At a low wind speed, small change occurs in the configuration with a small bending angle (Mode 1). The cylinders are divided into groups of two or three cylinders that exhibit damped oscillating motion (Mode 2). High wind speeds induce chaotic motion and deviation from in-line arrangement (Mode 3)

3.5 Tandem configuration of multiple cylinders

Fig. 8 shows variations of the average bending angle, drag reduction ratio, and average displacement with respect to Re in the case of three cylinders. T1 and T2 in Fig. 8(a) represent the group of two upstream cylinders and the remaining downstream cylinder respectively. The T1 and T2 groups show different phasic motions. For comparison, the corresponding results of a single cylinder are included in Fig. 8. The T1 group has the lowest average bending angle. The difference in bending angles of the T2 and a single cylinder increases as Re increases, which results from the wind reduction effect of the T1 group (Fig. 8(b)). In addition, the drag reduction ratio of the T1 and T2 groups is smaller than that of a single cylinder (Fig. 8(c)). In the co-shedding regime, the vortices shed from the T1 group increases the bending displacement of the T2 group. Therefore, the distance between the T1 and T2 groups increases. When the distance between T1 and T2 exceeds $5D$ (co-shedding regime), the separated shear layers roll up alternately, forming a vortex street in the gap between the two groups and behind the cylinders. Consequently, the T2 group of two downstream cylinders is displaced more than a single cylinder because the effect of vortex shedding is rather higher than the effect of reduced wind velocity.

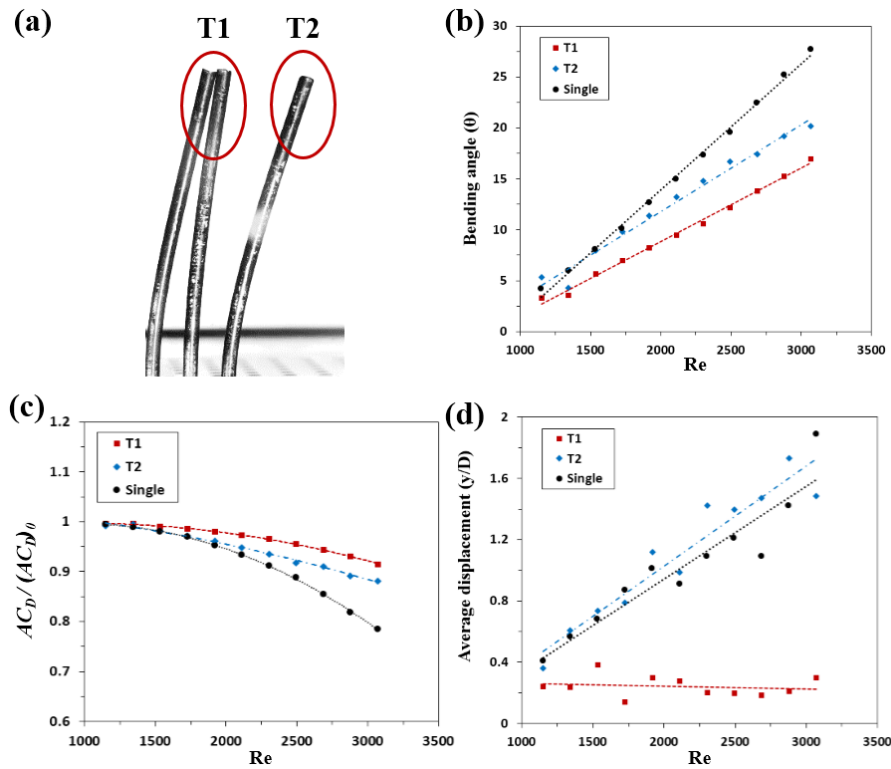


Fig. 8 (a) Three cylinders are reconfigured into two groups: T1 group represents the two upstream cylinders and T2 group denotes the single downstream cylinder. Variations of (b) bending angle, (c) drag reduction ratio, and (d) average displacement with respect to Re . Results for a single cylinder are included as a reference

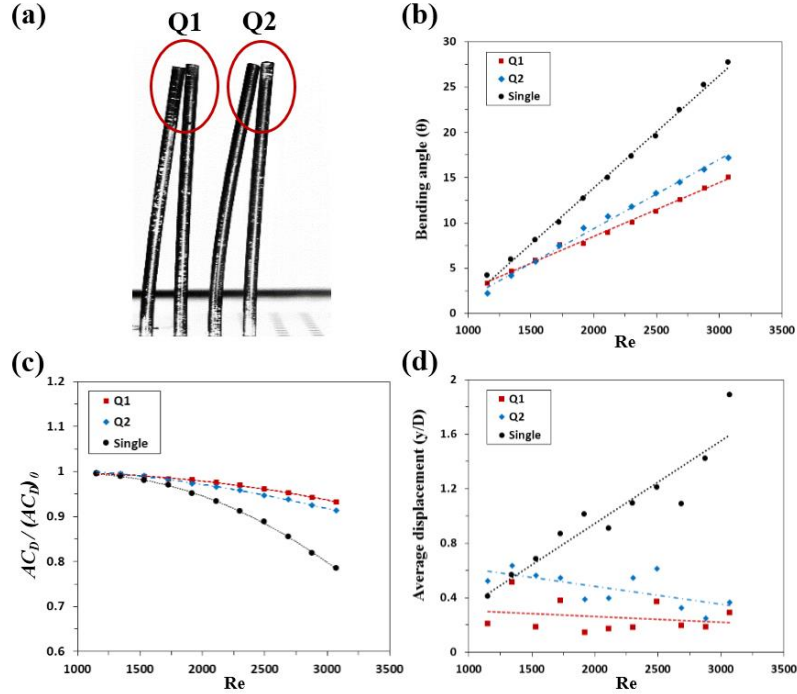


Fig. 9 (a) Four cylinders are reconfigured into two groups: Q1 group represents the two upstream cylinders and Q2 group indicates the two downstream cylinders. Variations of (b) bending angle, (c) drag reduction ratio, and (d) average displacement with respect to Re . Results for a single cylinder are included as a reference

Fig. 9 compares the oscillating motions of four cylinders (quad) with that of a single cylinder. Four cylinders arranged in-line are divided into the Q1 group of two upstream cylinders and the Q2 group of two downstream cylinders (Fig. 9(a)). The average bending angle and average displacement of the Q1 and Q2 groups are smaller than those of a single cylinder. The bending angle of the Q2 group is slightly higher than that of the Q1 group when $Re \geq 1920$ (Fig. 9(b)). The drag reduction ratio of the Q1 and Q2 groups becomes relatively smaller than that of a single cylinder as Re increases (Fig. 9(c)). The differences in average bending angle and average displacement of single and four cylinders also increase as the Re increases. The tendencies of the average bending angle and average displacement of the four-cylinder group are very similar to those of the two-cylinder group because both the Q1 and Q2 groups consist of two cylinders and have similar damping effects. However, the average bending angle and average displacement of the Q2 group are slightly higher than those of the Q1 group because of vortex shedding in the co-shedding zone.

Fig. 11 shows the variations of average displacement with respect to the number of cylinders consisting of a group at $Re = 2495$. For comparison, the average displacements of a single cylinder and the remaining downstream cylinders are also included. Average displacements of the single, T2, and P3 groups have relatively large values, ranging from 0.96 to 1.4. Although both T2 and P3 groups are affected by the vortices shed from upstream cylinders, the average displacement of P3

is smaller than that of a single cylinder. This result is attributed to the lateral motion of the P3 group. As the number of grouping cylinders increases, the average displacement has a general decreasing tendency because of the damping effect. A group consisting of two cylinders is classified into two different types, depending on the position of the upstream and downstream cylinders: upstream group (double, Q1, and P1) and downstream group (Q2, P2). The displacements of downstream two-cylinder groups are relatively larger than those of upstream two-cylinder groups due to the vortex shedding effect. On the other hand, three-cylinder groups have relatively small displacement because of the damping effect.

A group of flexible cylinders formed by aerodynamic features behave like a single body. Thus, average bending and displacement are significantly reduced compared to those of a single cylinder due to damping effect. Bending and displacement of a flexible plant stem are closely related to the fracture of the stem. Although the bending of flexible vegetation leads to the reduction of drag force (Vogel 1989), the relatively large bending and displacement of the stem give rise to fatigue and fracture. A vegetation with flexible stem and high vegetation density (small distance between individual plants), such as a reed colony, may induce a decrease in bending and displacement because a group of flexible plants under aerodynamic conditions moves like a single body, as demonstrated by the flexible cylinders discussed in the current study. Therefore, it is reasonable to infer that the probability of a flexible stem fracture is largely reduced as the plants form groups. The dynamic behaviors of flexible cylinders according to aerodynamic conditions can provide new insights into understanding the survival strategy of flexible vegetation, such as a reed colony.

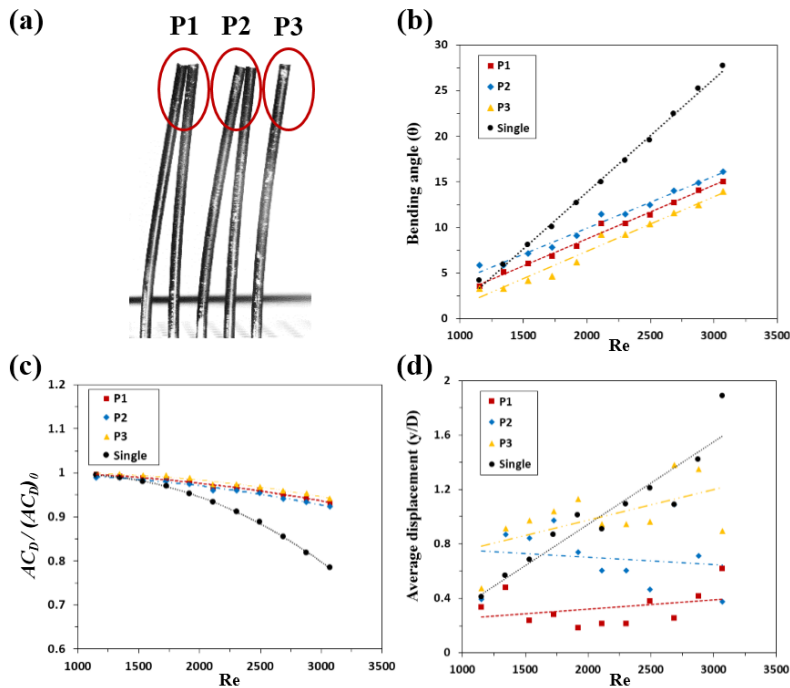


Fig. 10 (a) Five cylinders are reconfigured into these groups: P1 group represents the two upstream cylinders, P2 group indicates the next two cylinders, and P3 group is the single downstream cylinder. Variations of (b) bending angle, (c) drag reduction ratio, and (d) average displacement with respect to Re . Results for a single cylinder are included as a reference

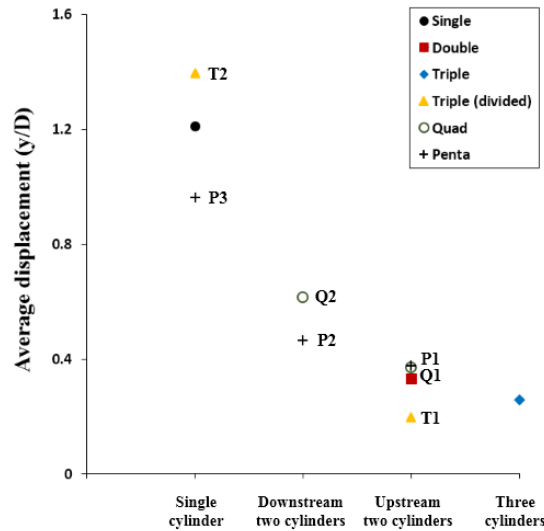


Fig. 11 Variation of average displacement according to the reconfiguration types of flexible cylinders at $Re = 2495$

4. Conclusions

The dynamic motions of flexible cylinders bio-inspired from a reed colony were investigated experimentally. Given that the Young's modulus of a PDMS cylinder is similar to that of a reed and a similar bending tendency is observed with respect to Re , the motions of a reed colony are studied using flexible cylinders. In the case of a single cylinder, both bending angle and average displacement are increased as the Re increases. On the other hand, multiple flexible cylinders arranged in-line induce a tandem configuration. The tandem groups of two and three cylinders in the extended-body regime oscillate as a group. As the Re increases, the drag reduction ratio $[AC_D/(AC_D)_0]$ of cylinders in a group is smaller than that of a single cylinder. This phenomenon is attributed to the fact that the first cylinder in the groups is supported by the downstream cylinders, which have a bending angle smaller than that of a single cylinder. In addition, the average displacement of tandem cylinders is significantly decreased as the Re increases compared to that of a single cylinder. In the case of multiple cylinders consisting of three to five cylinders, the tandem configuration is divided into two or three groups with different oscillation characteristics. The groups of downstream cylinders exhibit relatively large bending angle and displacement because of the vortices shed from the upstream cylinders in the co-shedding regime. However, both bending angle and displacement of these groups are significantly smaller than those of a single cylinder. Consequently, when the number of cylinders comprising a group increases, the tendency of displacement decreases because of the damping effect caused by the supporting downstream cylinders. The present results would provide a better understanding on the survival strategy of the reed colony with flexible stems.

Acknowledgments

This work was supported by the National Research Foundation of Korea (NRF) grant funded by the Korea government (MSIP) (No. 2008-0061991).

References

- Aiba, S. and Yamazaki, Y. (1976), "An experimental investigation of heat transfer around a tube in a bank", *J. Heat Transfer.*, **98**(3), 503-508.
- Alben, S., Shelley, M. and Zhang, J. (2002), "Drag reduction through self-similar bending of a flexible body", *Nature*, **420**(6915), 479-481.
- Bearman, P.W. (1984), "Vortex shedding from oscillating bluff bodies", *Annu. Rev. Fluid Mech.*, **16**(1), 195-222.
- de Langre, E. (2008), "Effects of wind on plants", *Ann. Rev. Fluid Mech.*, **40**(1), 141-168.
- Gosselin, F., de Langre, E. and Machado-Almeida, B.A. (2010), "Drag reduction of flexible plates by reconfiguration", *J. Fluid Mech.*, **650**, 319-341.
- Hetz, A.A., Dhaubhadel, M.N. and Telionis, D.P. (1991), "Vortex shedding over five in-line cylinders", *J. Fluid. Struct.*, **5**(3), 243-257.
- Huera-Huarte, F.J. and Bearman, P.W. (2009), "Wake structures and vortex-induced vibrations of a long flexible cylinder—Part 1: Dynamic response", *J. Fluid. Struct.*, **25**(6), 969-990.
- Huera-Huarte, F.J. and Bearman, P.W. (2011), "Vortex and wake-induced vibrations of a tandem arrangement of two flexible circular cylinders with near wake interference", *J. Fluid. Struct.*, **27**(2), 193-211.
- Huera-Huarte, F.J. and Gharib, M. (2011), "Vortex- and wake-induced vibrations of a tandem arrangement of two flexible circular cylinders with far wake interference", *J. Fluid. Struct.*, **27**(5-6), 824-828.
- Igarashi, T. (1986), "Characteristics of the flow around four circular cylinders arranged in line", *Bulletin of the JSME*, **29**(249), 751-757.
- Igarashi, T. and Suzuki, K. (1984), "Characteristics of the flow around three circular cylinders arranged in line", *Bulletin of the JSME*, **27**(233), 2397-2404.
- Sarpkaya, T. (2004), "A critical review of the intrinsic nature of vortex-induced vibrations", *J. Fluid. Struct.*, **19**(4), 389-447.
- Spatz, H.C., Beismann, H., Bruchert, F., Emanns, A. and Speck, T. (1997), "Biomechanics of the giant reed *Arundo donax*", *Phil. Trans. R. Soc. B.*, **352**(1349), 1-10.
- Speck, O. and Spatz, H.C. (2004), "Damped oscillations of the giant reed *Arundo donax* (Poaceae)", *Am. J. Botany.*, **91**(6), 789-796.
- Sumner, D. (2010), "Two circular cylinders in cross-flow: A review", *J. Fluid. Struct.*, **26**(6), 849-899.
- Vogel, S. (1989), "Drag and reconfiguration of broad leaves in high winds", *J. Exp. Botany.*, **40**(8), 941-948.
- Williamson, C.H.K. and Govardhan, R. (2004), "Vortex-induced vibrations", *Annu. Rev. Fluid Mech.*, **36**, 413-455.
- Xu, G. and Zhou, Y. (2004), "Strouhal numbers in the wake of two inline cylinders", *Exp. Fluids*, **37**(2), 248-256.
- Zdravkovich, M.M. (1977), "Review of flow interference between two circular cylinders in various arrangements", *J. Fluid. Eng. -TASME*, **99**(4), 618-633.
- Zdravkovich, M.M. (1987), "The effects of interference between circular cylinders in cross flow", *J. Fluid. Struct.*, **1**(2), 239-261.
- Zhou, Y. and Yiu, M.W. (2006), "Flow structure, momentum and heat transport in a two-tandem-cylinder

wake”, *J. Fluid Mech.*, **548** 17-48.

CC